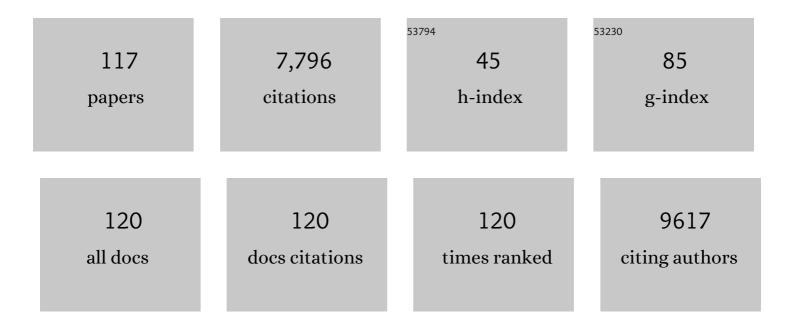
List of Publications by Year in descending order

Source: https://exaly.com/author-pdf/6224164/publications.pdf Version: 2024-02-01



#	Article	IF	CITATIONS
1	Heteroatom-doped graphene materials: syntheses, properties and applications. Chemical Society Reviews, 2014, 43, 7067-7098.	38.1	1,547
2	Ti <sub>3</sub> C <sub>2</sub> T <sub>X</sub> MXene for Sensing Applications: Recent Progress, Design Principles, and Future Perspectives. ACS Nano, 2021, 15, 3996-4017.	14.6	361
3	Hybrid Fibers Made of Molybdenum Disulfide, Reduced Graphene Oxide, and Multiâ€Walled Carbon Nanotubes for Solid‧tate, Flexible, Asymmetric Supercapacitors. Angewandte Chemie - International Edition, 2015, 54, 4651-4656.	13.8	334
4	Self-powered, visible-light photodetector based on thermally reduced graphene oxide–ZnO (rGO–ZnO) hybrid nanostructure. Journal of Materials Chemistry, 2012, 22, 2589-2595.	6.7	285
5	Design of Amorphous Manganese Oxide@Multiwalled Carbon Nanotube Fiber for Robust Solid-State Supercapacitor. ACS Nano, 2017, 11, 444-452.	14.6	216
6	High-Performance Foam-Shaped Strain Sensor Based on Carbon Nanotubes and Ti <sub>3</sub> C <sub>2</sub> T <sub><i>x</i></sub> MXene for the Monitoring of Human Activities. ACS Nano, 2021, 15, 9690-9700.	14.6	191
7	Layer-by-layer printing of laminated graphene-based interdigitated microelectrodes for flexible planar micro-supercapacitors. Electrochemistry Communications, 2015, 51, 33-36.	4.7	169
8	A Solid‣tate Fibriform Supercapacitor Boosted by Host–Guest Hybridization between the Carbon Nanotube Scaffold and MXene Nanosheets. Small, 2018, 14, e1801203.	10.0	158
9	Electrostatically Assembling 2D Nanosheets of MXene and MOFâ€Derivatives into 3D Hollow Frameworks for Enhanced Lithium Storage. Small, 2019, 15, e1904255.	10.0	138
10	Ultrasensitive Anti-Interference Voice Recognition by Bio-Inspired Skin-Attachable Self-Cleaning Acoustic Sensors. ACS Nano, 2019, 13, 13293-13303.	14.6	122
11	Fabrication of Ultralong Hybrid Microfibers from Nanosheets of Reduced Graphene Oxide and Transitionâ€Metal Dichalcogenides and their Application as Supercapacitors. Angewandte Chemie - International Edition, 2014, 53, 12576-12580.	13.8	119
12	Polyaniline-Decorated Supramolecular Hydrogel with Tough, Fatigue-Resistant, and Self-Healable Performances for All-In-One Flexible Supercapacitors. ACS Applied Materials & Interfaces, 2020, 12, 9736-9745.	8.0	119
13	All-Graphene-Based Highly Flexible Noncontact Electronic Skin. ACS Applied Materials & Interfaces, 2017, 9, 44593-44601.	8.0	110
14	Achieving stable and efficient water oxidation by incorporating NiFe layered double hydroxide nanoparticles into aligned carbon nanotubes. Nanoscale Horizons, 2016, 1, 156-160.	8.0	99
15	Rational Design of a Flexible CNTs@PDMS Film Patterned by Bioâ€Inspired Templates as a Strain Sensor and Supercapacitor. Small, 2019, 15, e1805493.	10.0	91
16	Singleâ€Step Selective Laser Writing of Flexible Photodetectors for Wearable Optoelectronics. Advanced Science, 2018, 5, 1800496.	11.2	87
17	Constructing a Low-Impedance Interface on a High-Voltage LiNi <sub>0.8</sub> Co <sub>0.1</sub> Mn <sub>0.1</sub> O <sub>2</sub> Cathode with 2,4,6-Triphenyl Boroxine as a Film-Forming Electrolyte Additive for Li-Ion Batteries. ACS Applied Materials & Interfaces. 2020, 12, 37013-37026.	8.0	86
18	Stabilizing LiCoO <sub>2</sub> /Graphite at High Voltages with an Electrolyte Additive. ACS Applied Materials & Interfaces, 2019, 11, 17940-17951.	8.0	83

#	Article	IF	CITATIONS
19	Sensitive fiber microelectrode made of nickel hydroxide nanosheets embedded in highly-aligned carbon nanotube scaffold for nonenzymatic glucose determination. Sensors and Actuators B: Chemical, 2018, 257, 23-28.	7.8	80
20	Tuning Array Morphology for Highâ€Strength Carbonâ€Nanotube Fibers. Small, 2010, 6, 132-137.	10.0	79
21	Gas sensing enhancing mechanism via doping-induced oxygen vacancies for gas sensors based on indium tin oxide nanotubes. Sensors and Actuators B: Chemical, 2018, 265, 273-284.	7.8	77
22	Electrochemically Mediated Surface-Initiated de Novo Growth of Polymers for Amplified Electrochemical Detection of DNA. Analytical Chemistry, 2017, 89, 9253-9259.	6.5	73
23	Surface strain-enhanced MoS2 as a high-performance cathode catalyst for lithium–sulfur batteries. EScience, 2022, 2, 405-415.	41.6	70
24	Dual-Function Metal–Organic Framework-Based Wearable Fibers for Gas Probing and Energy Storage. ACS Applied Materials & Interfaces, 2018, 10, 2837-2842.	8.0	68
25	Conductive regenerated silk-fibroin-based hydrogels with integrated high mechanical performances. Journal of Materials Chemistry B, 2019, 7, 1708-1715.	5.8	68
26	Preparation of Weavable, Allâ€Carbon Fibers for Nonâ€Volatile Memory Devices. Angewandte Chemie - International Edition, 2013, 52, 13351-13355.	13.8	67
27	Ultrathin and large-sized vanadium oxide nanosheets mildly prepared at room temperature for high performance fiber-based supercapacitors. Journal of Materials Chemistry A, 2017, 5, 2483-2487.	10.3	66
28	Highly Concentrated, Ultrathin Nickel Hydroxide Nanosheet Ink for Wearable Energy Storage Devices. Advanced Materials, 2017, 29, 1703455.	21.0	62
29	Polarity-assisted formation of hollow-frame sheathed nitrogen-doped nanofibrous carbon for supercapacitors. Nanoscale, 2019, 11, 2492-2500.	5.6	62
30	Oxygen vacancy enriched hollow cobaltosic oxide frames with ultrathin walls for efficient energy storage and biosensing. Nanoscale, 2018, 10, 21006-21012.	5.6	60
31	Design of a wearable and shape-memory fibriform sensor for the detection of multimodal deformation. Nanoscale, 2018, 10, 118-123.	5.6	58
32	Microfiber devices based on carbon materials. Materials Today, 2015, 18, 215-226.	14.2	57
33	Recent Advances in Design of Flexible Electrodes for Miniaturized Supercapacitors. Small Methods, 2020, 4, 1900824.	8.6	56
34	ldentifying the active site of ultrathin NiCo LDH as an efficient peroxidase mimic with superior substrate affinity for sensitive detection of hydrogen peroxide. Journal of Materials Chemistry B, 2019, 7, 6232-6237.	5.8	55
35	A modified Weibull model for tensile strength distribution of carbon nanotube fibers with strain rate and size effects. Applied Physics Letters, 2012, 101, .	3.3	52
36	Electrochemical capacitive properties of CNT fibers spun from vertically aligned CNT arrays. Journal of Solid State Electrochemistry, 2012, 16, 1775-1780.	2.5	52

#	Article	IF	CITATIONS
37	Holey nickel hydroxide nanosheets for wearable solid-state fiber-supercapacitors. Nanoscale, 2018, 10, 5442-5448.	5.6	50
38	Covalent organic framework-regulated ionic transportation for high-performance lithium-ion batteries. Journal of Materials Chemistry A, 2019, 7, 26540-26548.	10.3	48
39	Scalable preparation of high performance fibrous electrodes with bio-inspired compact core-fluffy sheath structure for wearable supercapacitors. Carbon, 2020, 157, 106-112.	10.3	48
40	Microstructure Design of Carbonaceous Fibers: A Promising Strategy toward Highâ€Performance Weaveable/Wearable Supercapacitors. Small, 2020, 16, e2000653.	10.0	48
41	Actuation triggered exfoliation of graphene oxide at low temperature for electrochemical capacitor applications. Carbon, 2014, 68, 748-754.	10.3	47
42	Weavable, Highâ€Performance, Solidâ€State Supercapacitors Based on Hybrid Fibers Made of Sandwiched Structure of MWCNT/rGO/MWCNT. Advanced Electronic Materials, 2016, 2, 1600102.	5.1	47
43	Constructing optimized three-dimensional electrochemical interface in carbon nanofiber/carbon nanotube hierarchical composites for high-energy-density supercapacitors. Carbon, 2017, 111, 502-512.	10.3	47
44	Highly sensitive detection of hydrogen peroxide at a carbon nanotube fiber microelectrode coated with palladium nanoparticles. Mikrochimica Acta, 2014, 181, 63-70.	5.0	46
45	Cooperative chemisorption of polysulfides via 2D hexagonal WS2-rimmed Co9S8 heterostructures for lithium–sulfur batteries. Chemical Engineering Journal, 2020, 392, 123734.	12.7	45
46	Revisiting Charge Storage Mechanism of Reduced Graphene Oxide in Zinc Ion Hybrid Capacitor beyond the Contribution of Oxygen ontaining Groups. Advanced Functional Materials, 2022, 32, .	14.9	45
47	Direct storage of holes in ultrathin Ni(OH) <sub>2</sub> on Fe <sub>2</sub> O <sub>3</sub> photoelectrodes for integrated solar charging battery-type supercapacitors. Journal of Materials Chemistry A, 2018, 6, 21360-21367.	10.3	44
48	Ammonium Intercalation Induced Expanded 1T-Rich Molybdenum Diselenides for Improved Lithium Ion Storage. ACS Applied Materials & Interfaces, 2021, 13, 17459-17466.	8.0	42
49	Load-transfer efficiency and mechanical reliability of carbon nanotube fibers under low strain rates. International Journal of Plasticity, 2013, 40, 56-64.	8.8	41
50	Robust wire-based supercapacitors based on hierarchical α-MoO 3 nanosheet arrays with well-aligned laminated structure. Chemical Engineering Journal, 2017, 320, 34-42.	12.7	41
51	In Situ Fabrication of Ni <sub>2</sub> P Nanoparticles Embedded in Nitrogen and Phosphorus Codoped Carbon Nanofibers as a Superior Anode for Li-Ion Batteries. ACS Sustainable Chemistry and Engineering, 2018, 6, 14795-14801.	6.7	41
52	Deciphering the catalysis essence of vanadium self-intercalated two-dimensional vanadium sulfides (V5S8) on lithium polysulfide towards high-rate and ultra-stable Li-S batteries. Energy Storage Materials, 2021, 43, 471-481.	18.0	38
53	Clothing polymer fibers with well-aligned and high-aspect ratio carbon nanotubes. Nanoscale, 2013, 5, 2870.	5.6	37
54	The incorporation of expanded 1T-enriched MoS2 boosts hybrid fiber improved charge storage capability. Carbon, 2020, 170, 543-549.	10.3	35

#	Article	IF	CITATIONS
55	Reliable and Large Curvature Actuation from Gradient-Structured Graphene Oxide. Journal of Physical Chemistry C, 2011, 115, 23741-23744.	3.1	34
56	Ultra-sensitive and wide-dynamic-range sensors based on dense arrays of carbon nanotube tips. Nanoscale, 2011, 3, 4854.	5.6	34
57	Design of Vertically Aligned Two-Dimensional Heterostructures of Rigid Ti <sub>3</sub> C <sub>2</sub> T <sub>X</sub> MXene and Pliable Vanadium Pentoxide for Efficient Lithium Ion Storage. ACS Nano, 2022, 16, 5556-5565.	14.6	33
58	Tough, Transparent, and Anti-Freezing Nanocomposite Organohydrogels with Photochromic Properties. ACS Applied Materials & amp; Interfaces, 2021, 13, 31180-31192.	8.0	32
59	Recent Advances in Molybdenum-Based Materials for Lithium-Sulfur Batteries. Research, 2021, 2021, 5130420.	5.7	31
60	Universal Strategy for Preparing Highly Stable PBA/Ti <sub>3</sub> C <sub>2</sub> T <sub><i>x</i></sub> MXene toward Lithium-Ion Batteries <i>via</i> Chemical Transformation. ACS Applied Materials & Interfaces, 2022, 14, 15298-15306.	8.0	30
61	Mechanistic insight in site-selective and anisotropic etching of prussian blue analogues toward designable complex architectures for efficient energy storage. Nanoscale, 2020, 12, 11112-11118.	5.6	29
62	Elastic organic crystals with ultralong phosphorescence for flexible anti-counterfeiting. Npj Flexible Electronics, 2021, 5, .	10.7	29
63	Hybrid fibers assembled from MoSe2/graphene heterostructures endow improved supercapacitive performance. Carbon, 2022, 187, 165-172.	10.3	29
64	Transition metal dichalcogenide/multi-walled carbon nanotube-based fibers as flexible electrodes for electrocatalytic hydrogen evolution. Chemical Communications, 2020, 56, 5131-5134.	4.1	28
65	Solution-Processed Sensing Textiles with Adjustable Sensitivity and Linear Detection Range Enabled by Twisting Structure. ACS Applied Materials & Interfaces, 2020, 12, 12155-12164.	8.0	28
66	Energy storage mechanism in aqueous fiber-shaped Li-ion capacitors based on aligned hydrogenated-Li <sub>4</sub> Ti <sub>5</sub> O <sub>12</sub> nanowires. Nanoscale, 2017, 9, 8192-8199.	5.6	26
67	Twist induced plasticity and failure mechanism of helical carbon nanotube fibers under different strain rates. International Journal of Plasticity, 2018, 110, 74-94.	8.8	26
68	Assembling laminated films <i>via</i> the synchronous reduction of graphene oxide and formation of copper-based metal organic frameworks. Journal of Materials Chemistry A, 2019, 7, 107-111.	10.3	26
69	Jahn–Teller distortions boost the ultrahigh areal capacity and cycling robustness of holey NiMn-hydroxide nanosheets for flexible energy storage devices. Nanoscale, 2020, 12, 22075-22081.	5.6	26
70	Ultrastable lithium–sulfur batteries with outstanding rate capability boosted by NiAs-type vanadium sulfides. Journal of Materials Chemistry A, 2020, 8, 18358-18366.	10.3	26
71	Tough Interfacial Adhesion of Bilayer Hydrogels with Integrated Shape Memory and Elastic Properties for Controlled Shape Deformation. ACS Applied Materials & Interfaces, 2021, 13, 10457-10466.	8.0	26
72	Solutionâ€Processable Design of Fiberâ€Shaped Wearable Zn//Ni(OH) <sub>2</sub> Battery. Energy Technology, 2018, 6, 2326-2332.	3.8	24

#	Article	IF	CITATIONS
73	One-pot sulfur-containing ion assisted microwave synthesis of reduced graphene oxide@nano-sulfur fibrous hybrids for high-performance lithium-sulfur batteries. Electrochimica Acta, 2019, 325, 134920.	5.2	24
74	General Metal-Ion Mediated Method for Functionalization of Graphene Fiber. ACS Applied Materials & Interfaces, 2017, 9, 37022-37030.	8.0	23
75	Ultrathin NiMn layered double hydroxide nanosheets with a superior peroxidase mimicking performance to natural HRP for disposable paper-based bioassays. Journal of Materials Chemistry B, 2021, 9, 983-991.	5.8	22
76	Polarization behaviors of twisted carbon nanotube fibers. Journal of Raman Spectroscopy, 2012, 43, 1221-1226.	2.5	21
77	Dissymmetric interface design of SnO2/TiO2 side-by-side bi-component nanofibers as photoanodes for dye sensitized solar cells: Facilitated electron transport and enhanced carrier separation. Journal of Colloid and Interface Science, 2021, 583, 24-32.	9.4	21
78	Probing structure and strain transfer in dry-spun carbon nanotube fibers by depth-profiled Raman spectroscopy. Applied Physics Letters, 2013, 103, .	3.3	20
79	Engineering the Li Storage Properties of Graphene Anodes: Defect Evolution and Pore Structure Regulation. ACS Applied Materials & Interfaces, 2016, 8, 33712-33722.	8.0	20
80	"Rose Flowers―assembled from mesoporous NiFe2O4 nanosheets for energy storage devices. Journal of Materials Science: Materials in Electronics, 2017, 28, 14058-14068.	2.2	20
81	Effect of TiO <sub>2</sub> -rGO heterojunction on electron collection efficiency and mechanical properties of fiber-shaped dye-sensitized solar cells. Journal Physics D: Applied Physics, 2019, 52, 095502.	2.8	20
82	Tunable white light emission by variation of composition and defects of electrospun Al <sub>2</sub> O <sub>3</sub> –SiO <sub>2</sub> nanofibers. Beilstein Journal of Nanotechnology, 2015, 6, 313-320.	2.8	19
83	A Capacitorâ€ŧype Faradaic Junction for Direct Solar Energy Conversion and Storage. Angewandte Chemie - International Edition, 2021, 60, 1390-1395.	13.8	19
84	Mesh-like vertical structures enable both high areal capacity and excellent rate capability. Journal of Energy Chemistry, 2021, 53, 226-233.	12.9	18
85	Reversible Charge Transfer and Adjustable Potential Window in Semiconductor/Faradaic Layer/Liquid Junctions. IScience, 2020, 23, 100949.	4.1	17
86	Amorphous phase induced high phosphorous-doping in dandelion-like cobalt sulfides for enhanced battery-supercapacitor hybrid device. Journal of Electroanalytical Chemistry, 2021, 889, 115231.	3.8	17
87	Interface/defect-tuneable macro and micro photoluminescence behaviours of trivalent europium ions in electrospun ZrO <sub>2</sub> /ZnO porous nanobelts. Physical Chemistry Chemical Physics, 2017, 19, 9223-9231.	2.8	16
88	A facile grinding approach to embed red phosphorus in N,P-codoped hierarchical porous carbon for superior lithium storage. Science China Materials, 2020, 63, 55-61.	6.3	16
89	Near-infrared responsive shape memory hydrogels with programmable and complex shape-morphing. Science China Technological Sciences, 2021, 64, 1752-1764.	4.0	15
90	Stiffness Engineering of Ti <sub>3</sub> C <sub>2</sub> T <i><sub>X</sub></i> MXeneâ€Based Skinâ€Inspired Pressure Sensor with Broadâ€Range Ultrasensitivity, Low Detection Limit, and Gas Permeability. Advanced Materials Interfaces, 2022, 9, .	3.7	15

#	Article	IF	CITATIONS
91	Trench structure assisted alignment in ultralong and dense carbon nanotube arrays. Journal of Materials Chemistry C, 2015, 3, 2215-2222.	5.5	14
92	Hierarchically tubular architectures composed of vertical carbon nanosheets embedded with oxygen-vacancy enriched hollow Co3O4 nanoparticles for improved energy storage. Electrochimica Acta, 2020, 356, 136843.	5.2	14
93	The Jahn-Teller Effect for Amorphization of Molybdenum Trioxide towards High-Performance Fiber Supercapacitor. Research, 2021, 2021, 6742715.	5.7	14
94	Construction of all-carbon micro/nanoscale interconnected sulfur host for high-rate and ultra-stable lithium-sulfur batteries: Role of oxygen-containing functional groups. Journal of Colloid and Interface Science, 2022, 608, 459-469.	9.4	13
95	High-Strength Albumin Hydrogels With Hybrid Cross-Linking. Frontiers in Chemistry, 2020, 8, 106.	3.6	12
96	Fe,N-doped carbon as peroxidase mimics for single-use colorimetric bioassays. Journal of Materials Science, 2021, 56, 13579-13589.	3.7	12
97	Highly Reliable Carbon Nanotubeâ€Based Composite Fibers Cross‣inked by a 3D Polymer Network. Advanced Engineering Materials, 2014, 16, 961-965.	3.5	11
98	Direct Preparation of Carbon Nanotube Intramolecular Junctions on Structured Substrates. Scientific Reports, 2016, 6, 38032.	3.3	11
99	Site-Selective Transformation for Preparing Tripod-like NiCo-Sulfides@Carbon Boosts Enhanced Areal Capacity and Cycling Reliability. ACS Applied Materials & amp; Interfaces, 2021, 13, 25316-25324.	8.0	11
100	Designing Tubular Architectures Composed of Hollow Nâ€Đoped Carbon Polyhedrons for Improved Supercapacitance. Advanced Materials Interfaces, 2021, 8, 2100805.	3.7	11
101	Enhanced Jahn–Teller distortion boosts molybdenum trioxide's superior lithium ion storage capability. Dalton Transactions, 2022, 51, 524-531.	3.3	11
102	2D material–based peroxidase-mimicking nanozymes: catalytic mechanisms and bioapplications. Analytical and Bioanalytical Chemistry, 2022, 414, 2971-2989.	3.7	11
103	Photovoltage memory effect in a portable Faradaic junction solar rechargeable device. Nature Communications, 2022, 13, 2544.	12.8	11
104	Mechanisms for selfâ€ŧemplating design of micro/nanostructures toward efficient energy storage. Exploration, 2022, 2, .	11.0	11
105	Highly enhanced electrochemical cycling stabilities of hierarchical partially-embedded MnO/carbon nanofiber composites as supercapacitor electrodes. Materials Science and Engineering B: Solid-State Materials for Advanced Technology, 2020, 262, 114684.	3.5	10
106	5-Carboxyfluorescein: intrinsic peroxidase-like catalytic activity and its application in the biomimetic synthesis of polyaniline nanoplatelets. Journal of Materials Chemistry B, 2017, 5, 5937-5941.	5.8	9
107	Time-dependent microstructural evolution mechanisms of twisted carbon nanotube fibers under tension and relaxation. International Journal of Plasticity, 2021, 136, 102866.	8.8	9
108	Wetâ€Chemistry: A Useful Tool for Deriving Metal–Organic Frameworks toward Supercapacitors and Secondary Batteries. Advanced Materials Interfaces, 2022, 9, .	3.7	9

#	Article	IF	CITATIONS
109	Co <sub>2</sub> V <sub>2</sub> O <sub>7</sub> @Ti <sub>3</sub> C <sub>2</sub> T <sub>x</sub> MXene Hollow Structures Synergizing the Merits of Conversion and Intercalation for Efficient Lithium Ion Storage. Advanced Sustainable Systems, 2022, 6, .	5.3	8
110	Nonlinear stress-strain behavior of carbon nanotube fibers subject to slow sustained strain rate. Applied Physics Letters, 2013, 103, .	3.3	7
111	Design of highly ordered hierarchical catalytic nanostructures as high-flexibility counter electrodes for fiber-shaped dye-sensitized solar cells. Applied Physics Letters, 2021, 118, .	3.3	7
112	Fabrication of Microscale Carbon Nanotube Fibers. Journal of Nanomaterials, 2012, 2012, 1-10.	2.7	6
113	A high-voltage solar rechargeable device based on a CoPi/BiVO <sub>4</sub> faradaic junction. Journal of Materials Chemistry A, 2022, 10, 1802-1807.	10.3	6
114	A Review on the Prediction of Health State and Serving Life of Lithiumâ€Ion Batteries. Chemical Record, 2022, 22, .	5.8	6
115	Tunable hierarchical hexagonal nickel telluride (Ni3Te2) laminated microsheets as flexible counter electrodes for high-performance fibrous dye-sensitized solar cells: Accelerated electrocatalysis reduction of I3â° ions. Chemical Engineering Journal, 2022, 442, 136286.	12.7	5
116	Dual Enhancement of Sodium Storage Induced through Both S-Compositing and Co-Doping Strategies. ACS Applied Materials & Interfaces, 2021, 13, 54043-54058.	8.0	3
117	A Capacitorâ€ŧype Faradaic Junction for Direct Solar Energy Conversion and Storage. Angewandte Chemie, 2021, 133, 1410-1415.	2.0	1